



REAL-TIME ESTIMATION OF VEHICLE INERTIA PARAMETERS BASED ON KALMAN-BUCY FILTER

Nguyen Tuan Anh

University of Transport and Communications, No 3 Cau Giay Street, Hanoi, Vietnam

ARTICLE INFO

TYPE: Research Article

Received: 13/04/2024

Revised: 04/05/2024

Accepted: 07/05/2024

Published online: 15/05/2024

<https://doi.org/10.47869/tcsj.75.4.10>

* *Corresponding author*

Email: nguyentuananh@utc.edu.vn; Tel: 0984023818

Abstract. Vehicle inertial parameters such as mass and moments of inertia are required for most vehicle dynamic control systems. Due to the wide range variation of these parameters during vehicle operation, accurate estimation of their values in real-time plays an important role in improving the efficiency of vehicle control systems. In this article, the vehicle sprung mass and moments of inertia are estimated in real-time based on a Kalman-Bucy filter algorithm designed for a spatial vibration model of a two-axle truck. This proposed method requires measuring only the vertical, roll, and pitch velocity of the sprung mass and, therefore can reduce the sensor cost significantly. The simulation results for a random roughness road profile according to ISO 8608 class C with step variations in sprung mass and moments of inertia showed that the designed estimator rejected the process and measurement noises and tracked the real vehicle parameters effectively with acceptable errors.

Keywords: sprung mass, moments of inertia, spatial vehicle model, real-time estimation, Kalman-Bucy filter.

@ 2024 University of Transport and Communications

1. INTRODUCTION

The inertia parameters of a vehicle, such as the sprung mass and roll and pitch moment of inertia, have a significant effect on vehicle ride handling, safety, and fuel consumption as well as the efficiency of vehicle dynamic control systems [1-3]. The nominal value of these parameters is usually measured off-line by commercial testbeds or calculated using mathematical approaches. However, depending on the various load conditions, the value of sprung mass and moments of inertia can be varied over a wide range. The difference between the actual value of vehicle inertia parameters and their assumption of constant value throughout all operating conditions results in a reduction in the accuracy and performance of control systems. Therefore, accurate identification of inertial parameters in real-time is a crucial role in improving the performance of vehicle control systems. Additionally, information on vehicle mass can be integrated with the vehicle monitoring device to help the transport companies and the transport administrations manage and control more effectively overloaded vehicles.

Generally, the approaches for estimating vehicle inertia parameters in real-time are based on various vehicle dynamics. The most common approach is based on longitudinal dynamics mainly applied to modern vehicles since it can use existing sensors installed. An example of mass estimation employs the vehicle engine torque, drive train inertia, wind resistance, rolling resistance, and road grade [3-6]. The problem as addressed by [3] is that the parameter estimation is highly sensitive to the estimation of the rolling resistance of the vehicle, a parameter that changes non-trivially over time. Using lateral dynamics is another approach for the estimation of vehicle parameters [2, 7]. Like the longitudinal dynamics-based approach, this method also requires multiple sensors available on the vehicle to measure the necessary signals. Valid information from the suspension could give good estimates of the inertia parameters of the sprung mass [8-11]. This requires some sort of sensing to measure either the relative displacement of the spring or the suspension force [8-10]. Therefore, the approach based on vertical dynamics can be seen as the most suitable choice for the estimation of vehicle inertia parameters without existing sensors installed.

While several estimation methods have been proposed in the literature, such as Kalman Filtering (KF) [3, 9], Extended Kalman Filtering (EKF) [7, 10], Recursive Least Squares (RLS) [6], and many others, none of them have seen widespread adoption in current vehicle technologies despite their potential to significantly improve automotive controls. The applications of the Kalman-Bucy filter (KBF) for estimating the vehicle inertia parameters or the state parameters of a vertical dynamics model have been introduced in [8, 11]. The mass and pitch moment of inertia of the vehicle sprung mass can be estimated using a KBF designed based on a half-car vertical vibration model with vertical accelerations of the front and rear axle are measured outputs [8].

This article introduces a KBF designed for a simplified spatial vehicle model that uses only the vertical, roll, and pitch velocity of the sprung mass as measured outputs to estimate the sprung mass and roll and pitch moment of inertia of a two-axle truck. The relative displacement and relative velocity of suspension at four wheels are treated as the system inputs instead of the road excitations. Thus the proposed method avoids the requirement of knowing or estimating the ground inputs. Simulation analysis and evaluation results implemented in Matlab Simulink with the designed KBF have demonstrated the effectiveness of the estimator in roughness road conditions with the step variations of the sprung mass inertia parameters in real time.

2. SPATIAL VIBRATION DYNAMICS OF VEHICLE

This section introduces a conventional 7 degree of freedom (DOF) spatial vibration model used for simulation as a real vehicle to gather vertical vibration signals of the sprung and un-sprung mass from road excitations. Those signals are then considered as the measured inputs of a simplified 3 DOF model employed to design the KBF estimator.

2.1. Conventional Spatial Vibration Model of Vehicle

The conventional model of spatial vibration of a two-axle truck described in Figure 1 consists of a rigid chassis (characterized by the sprung mass m_s , roll moment of inertia J_x , and pitch moment of inertia J_y) connected to the front and rear solid axle (characterized by the un-sprung masses m_{uf} , m_{ur} and roll moments of inertia J_{uf} , J_{ur} respectively) by four suspension systems (denoted by the spring stiffness c_{si} ($i = 1 \div 4$) and damping coefficient k_{si}) at the four wheels (denoted by the tire stiffness c_{ui}). For the model, it can be assumed that: 1) the wheels do not leave the road surface, 2) the suspension and tire characteristics are linear, 3) the roll and pitch angle are very small, and 4) the position of vehicle center of gravity is unchanged.

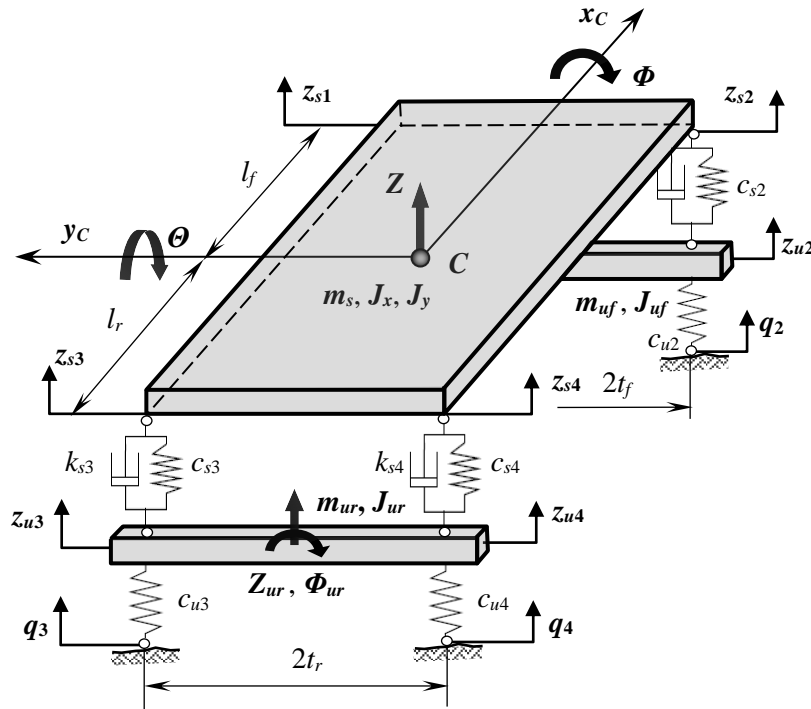


Figure 1. Conventional spatial vehicle model.

The model has 7 DOF: vertical displacement Z , pitch motion Θ and roll motion Φ of the sprung mass; vertical displacements Z_{uf} and Z_{ur} and roll motion Φ_{uf} and Φ_{ur} of the front and rear un-sprung mass, respectively. The model inputs are the road profiles q_i at the four wheels.

The equations of motion of the conventional spatial vehicle model corresponding to 7 DOF is written as follows:

$$\begin{cases} m_s \ddot{Z} = -(F_{s1} + F_{s2} + F_{s3} + F_{s4}), \\ J_x \ddot{\Phi} = -(t_f F_{s1} - t_f F_{s2} + t_r F_{s3} - t_r F_{s4}), \\ J_y \ddot{\Theta} = -(-l_f F_{s1} - l_f F_{s2} + l_r F_{s3} + l_r F_{s4}), \\ m_{uf} \ddot{Z}_{uf} = (F_{s1} + F_{s2}) - (F_{u1} + F_{u2}), \\ m_{ur} \ddot{Z}_{ur} = (F_{s3} + F_{s4}) - (F_{u3} + F_{u4}), \\ J_{uf} \ddot{\Phi}_{uf} = (F_{s1} - F_{s2}) t_f - (F_{u1} - F_{u2}) t_f, \\ J_{ur} \ddot{\Phi}_{ur} = (F_{s3} - F_{s4}) t_r - (F_{u3} - F_{u4}) t_r, \end{cases} \quad (1)$$

where the suspension force F_{si} and the tire force F_{ui} at the wheels is calculated by:

$$\begin{aligned} F_{si} &= k_{si} (\dot{z}_{si} - \dot{z}_{ui}) + c_{si} (z_{si} - z_{ui}), \\ F_{ui} &= c_{ui} (z_{ui} - q_i), \quad i = 1 \div 4. \end{aligned} \quad (2)$$

Let $\mathbf{x}_{01} = [z_1^T, \dot{z}_1^T]^T$ is the vector of states, here $z_1 = [Z, \Phi, \Theta, Z_{uf}, Z_{ur}, \Phi_{uf}, \Phi_{ur}]^T$ is the vector of generalized coordinates; $\mathbf{u}_{01} = [q_1, q_2, q_3, q_4]^T$ denotes the vector of inputs; and $\mathbf{y}_{01} = [\Delta z_s^T, \Delta \dot{z}_s^T]^T$ is the vector of outputs, where $\Delta z_s = (z_s - z_u)$ and $\Delta \dot{z}_s = (\dot{z}_s - \dot{z}_u)$ are the vectors of relative displacement and velocity between the sprung mass and un-sprung mass used as the inputs to the simplified model. Then the equations of motion of the conventional spatial model can be expressed in the state-space form:

$$\begin{cases} \dot{\mathbf{x}}_{01} = \mathbf{A}_{01} \mathbf{x}_{01} + \mathbf{B}_{01} \mathbf{u}_{01} \\ \mathbf{y}_{01} = \mathbf{C}_{01} \mathbf{x}_{01} + \mathbf{D}_{01} \mathbf{u}_{01}, \end{cases} \quad (3)$$

with the system matrices \mathbf{A}_{01} , \mathbf{B}_{01} , \mathbf{C}_{01} , and \mathbf{D}_{01} are defined by:

$$\begin{aligned} \mathbf{A}_{01} &= \begin{bmatrix} \mathbf{0}_{(7 \times 7)} & \mathbf{I}_{(7 \times 7)} \\ -\mathbf{M}_1^{-1} \mathbf{C}_1 & -\mathbf{M}_1^{-1} \mathbf{K}_1 \end{bmatrix}_{(14 \times 14)}, & \mathbf{B}_{01} &= \begin{bmatrix} \mathbf{0}_{(7 \times 4)} \\ \mathbf{M}_1^{-1} \mathbf{H}_1 \end{bmatrix}_{(14 \times 4)}, \\ \mathbf{C}_{01} &= \begin{bmatrix} \mathbf{G}_{fs(4 \times 7)} & \mathbf{0}_{(4 \times 7)} \\ \mathbf{0}_{(4 \times 7)} & \mathbf{G}_{fs(4 \times 7)} \end{bmatrix}_{(8 \times 14)}, & \mathbf{D}_{01} &= \begin{bmatrix} \mathbf{0}_{(8 \times 4)} \end{bmatrix}_{(8 \times 4)}, \end{aligned} \quad (4)$$

and other matrices are described as follow:

$$\begin{aligned} \mathbf{M}_1 &= \begin{bmatrix} \mathbf{M}_s & \mathbf{0} \\ \mathbf{0} & \mathbf{M}_u \end{bmatrix}, \quad \mathbf{M}_s = \text{diag}([m_s, J_x, J_y]), \quad \mathbf{M}_u = \text{diag}([m_{uf}, m_{ur}, J_{uf}, J_{ur}]), \\ \mathbf{C}_1 &= \begin{bmatrix} \mathbf{C}_{ss} \\ \mathbf{C}_{uu} \end{bmatrix}, \quad \mathbf{C}_{ss} = \mathbf{G}_s^T \mathbf{C}_s \mathbf{G}_{fs}, \quad \mathbf{C}_{uu} = -\mathbf{G}_u^T (\mathbf{C}_s \mathbf{G}_{fs} - \mathbf{C}_u \mathbf{G}_{fu}), \\ \mathbf{C}_s &= \text{diag}([c_{sf}, c_{sf}, c_{sr}, c_{sr}]), \quad \mathbf{C}_u = \text{diag}([c_{uf}, c_{uf}, c_{ur}, c_{ur}]), \\ \mathbf{K}_1 &= \begin{bmatrix} \mathbf{K}_{ss} \\ \mathbf{K}_{uu} \end{bmatrix}, \quad \mathbf{K}_{ss} = \mathbf{G}_s^T \mathbf{K}_s \mathbf{G}_{fs}, \quad \mathbf{K}_{uu} = -\mathbf{G}_u^T \mathbf{K}_s \mathbf{G}_{fs}, \quad \mathbf{K}_s = \text{diag}([k_{sf}, k_{sf}, k_{sr}, k_{sr}]), \end{aligned}$$

$$\begin{aligned}
 \mathbf{H}_1 &= \begin{bmatrix} \mathbf{0} \\ \mathbf{G}_u^T \mathbf{C}_u \end{bmatrix}, \\
 \mathbf{G}_s &= \begin{bmatrix} 1 & t_f & -l_f \\ 1 & -t_f & -l_f \\ 1 & t_r & l_r \\ 1 & -t_r & l_r \end{bmatrix}, \quad \mathbf{G}_u = \begin{bmatrix} 1 & 0 & t_f & 0 \\ 1 & 0 & -t_f & 0 \\ 0 & 1 & 0 & t_r \\ 0 & 1 & 0 & -t_r \end{bmatrix}, \quad \mathbf{G}_{fs} = [\mathbf{G}_s \quad -\mathbf{G}_u], \quad \mathbf{G}_{fu} = [\mathbf{0} \quad \mathbf{G}_u].
 \end{aligned} \tag{5}$$

All parameters of the model in Equation (5) are assumed to be known or predefined, therefore all matrices above are time invariant.

2.2. Simplified Vehicle Model

During operation, the variation in the vehicle load only changes the inertial parameters of the sprung mass, (including sprung mass m_s and moments of inertia J_x, J_y). In contrast, the inertial parameters of the un-sprung mass are unchanged. It is therefore possible to simplify the conventional spatial vehicle model to a simplified model of the sprung mass with the four vertical displacements of the unsprung masses as inputs as depicted in Figure 2. This reduces the computational complexity and removes the need for knowledge about the weight, stiffness, and damping coefficient of the wheels and knowledge about the road profile. Thus, the simplified vehicle model has only 3 DOF: vertical displacement Z , pitch motion Θ , and roll motion Φ of the sprung mass.

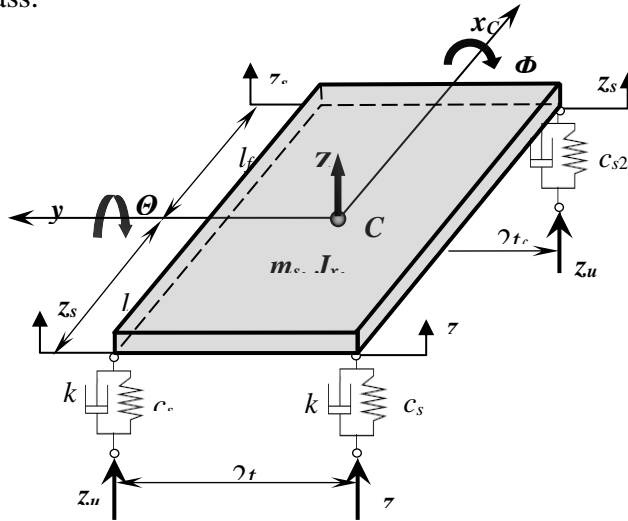


Figure 2. Simplified vehicle model.

Equations of motion of the simplified model are the first three lines in Equation (1), which can be expressed in the matrix form:

$$\mathbf{M}_s \ddot{\mathbf{z}}_2 = \mathbf{H}_2 \mathbf{y}_{01}, \tag{6}$$

where $\mathbf{z}_2 = [Z, \Phi, \Theta]^T$ is the vector of generalized coordinates of the simplified model and $\mathbf{H}_2 = \begin{bmatrix} -\mathbf{G}_s^T \mathbf{C}_s & -\mathbf{G}_s^T \mathbf{K}_s \end{bmatrix}$ is the excitation matrix.

Differing from the conventional model, the simplified model has three unknown parameters that have to be estimated in real-time and denoted by the vector of parameters $\mathbf{p} = [m_s, J_x, J_y]^T$.

To estimate these parameters via the KBF method, the state-space equation of the simplified model can be defined as follows:

$$\begin{cases} \dot{\mathbf{x}}_{02} = \mathbf{A}_{02} \mathbf{x}_{02} + \mathbf{B}_{02} \mathbf{u}_{02} \\ \mathbf{y}_{02} = \mathbf{C}_{02} \mathbf{x}_{02} + \mathbf{D}_{02} \mathbf{u}_{02}, \end{cases} \quad (7)$$

where:

$$\begin{aligned} \mathbf{x}_{02} &= [\dot{\mathbf{z}}_2^T, \mathbf{p}^T]^T = [\dot{Z}, \dot{\phi}, \dot{\theta}, m_s, J_x, J_y]^T_{(6 \times 1)}, \\ \mathbf{y}_{02} &= [\dot{Z}, \dot{\phi}, \dot{\theta}]^T_{(3 \times 1)}, \\ \mathbf{u}_{02} = \mathbf{y}_{01} &= [\Delta \mathbf{z}_s^T, \Delta \dot{\mathbf{z}}_s^T]^T_{(8 \times 1)}, \\ \mathbf{A}_{02} &= [\mathbf{0}]_{(6 \times 6)}, \quad \mathbf{B}_{02} = \begin{bmatrix} \mathbf{M}_s^{-1} \mathbf{H}_2 \\ \mathbf{0}_{(3 \times 8)} \end{bmatrix}_{(6 \times 8)}, \\ \mathbf{C}_{02} &= [\mathbf{I}_{(3 \times 3)} \quad \mathbf{0}_{(3 \times 3)}]_{(3 \times 6)}, \quad \mathbf{D}_{02} = [\mathbf{0}]_{(3 \times 8)}. \end{aligned} \quad (8)$$

It should be noted that since \mathbf{p} is time invariant, $\dot{\mathbf{p}} = \mathbf{0}$ in Equation (7).

3. KALMAN-BUCY FILTER DESIGN

The traditional Kalman filter (KF) is a discrete filter over time [3]. In practice, many cases require estimation of state parameters that cannot be directly measured by a system that varies continuously over time. Then it is necessary to design a continuous filter over time to replace the KF that continuously calculates the state parameters of the system. The Kaman-Bucy filter (KBF) can be considered the time-continuous filter of the KF [12].

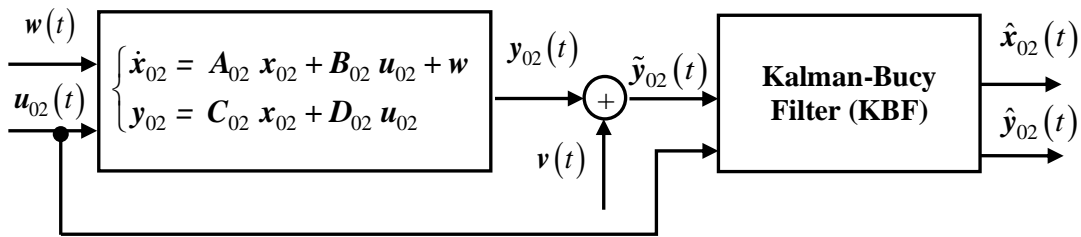


Figure 3. Diagram of the Kalman-Bucy filter for 3 DOF simplified model.

The diagram of the KBF for the 3 DOF simplified model is shown in Figure 3, where $\mathbf{u}_{02}(t)$ is the vector of inputs, $\mathbf{y}_{02}(t)$ and $\tilde{\mathbf{y}}_{02}(t)$ denote the vector of actual and measured process outputs, $\hat{\mathbf{x}}_{02}(t)$ and $\hat{\mathbf{y}}_{02}(t)$ stand for the estimated states and outputs. The vector $\mathbf{w}(t)$ and $\mathbf{v}(t)$ are random variable vectors representing process noise and measurement noise. These two random variables are independent of each other and are assumed to follow the Gaussian normal distribution with mean zero and the covariance matrix are \mathbf{Q} and \mathbf{R} , respectively: $\mathbf{w}(t) \sim N(0, \mathbf{Q})$, $\mathbf{v}(t) \sim N(0, \mathbf{R})$.

The task of the KBF is to estimate the unknown states with given inputs and measurable outputs. differ from the KF which uses a predictor-corrector algorithm to update the state estimates, the KBF requires integrating a differential Riccati equation through time. The filter update equations are given by [8,11,12]:

$$\begin{cases} \mathbf{K} = \mathbf{P} \mathbf{C}_{02}^T \mathbf{R}^{-1} \\ \dot{\hat{\mathbf{x}}}_{02} = \mathbf{A}_{02} \hat{\mathbf{x}}_{02} + \mathbf{B}_{02} \mathbf{u}_{02} + \mathbf{K} [\tilde{y}_{02} - (\mathbf{C}_{02} \hat{\mathbf{x}}_{02} + \mathbf{D}_{02} \mathbf{u}_{02})] \\ \hat{y}_{02} = \mathbf{C}_{02} \hat{\mathbf{x}}_{02} + \mathbf{D}_{02} \mathbf{u}_{02} \\ \dot{\mathbf{P}} = \mathbf{A}_{02} \mathbf{P} + \mathbf{P} \mathbf{A}_{02}^T - \mathbf{P} \mathbf{C}_{02}^T \mathbf{R}^{-1} \mathbf{C}_{02} \mathbf{P} + \mathbf{Q} \end{cases} \quad (9)$$

In the above \mathbf{K} is called the KBF observer gain matrix, \mathbf{P} denotes a covariance estimation matrix of the measurement error satisfying the Riccati equation, \mathbf{R} is the weighting matrix of measurement noises, and \mathbf{Q} is the weighting matrix of process noises. For KBF implementation both $\hat{\mathbf{x}}(t)$ and $\dot{\mathbf{P}}(t)$ must be integrated through time.

Figure 4 shows the block diagram for estimating the vehicle inertia parameters in Matlab Simulink with the KBF designed on the base of the 3 DOF simplified model. The block “Kalman-Bucy Filter” is an embedded Matlab function used to calculate the KBF algorithm in Equation (8), where “Filter State Out” contains both $\hat{\mathbf{x}}(t)$ and $\dot{\mathbf{P}}(t)$.

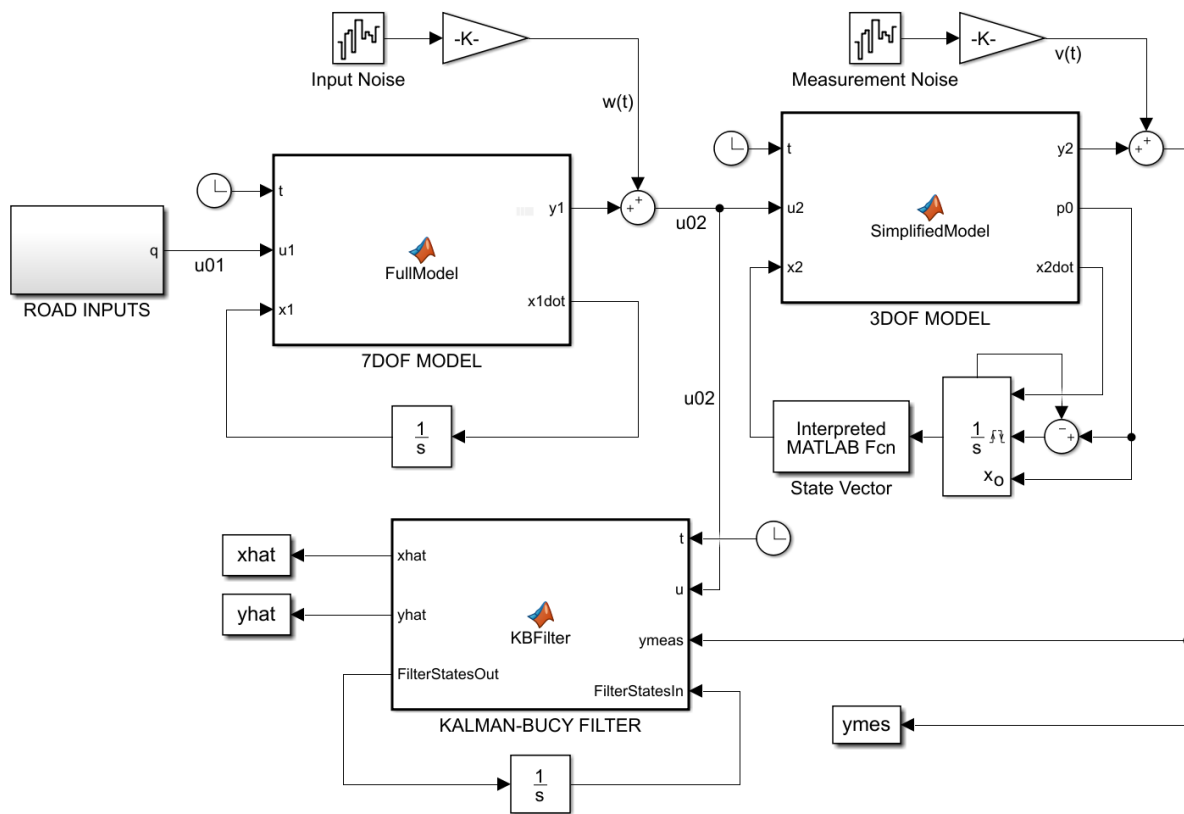


Figure 4. Kalman-Bucy filter for spatial vehicle model in Simulink.

4. SIMULATION AND EVALUATION

In this section, the KBF designed for the simplified spatial vehicle model is used to estimate the mass, roll moment of inertia, and pitch moment of inertia of the sprung mass. The vehicle parameter values are listed in Table 1, where the damping coefficient of the wheels is neglected, other parameters of the suspension system are identical for the left and right side. The system input is a random roughness road profile according to ISO 8608 class C [13] with differences between the two sides of the wheel. The magnitude value of the vector of process noise and

measurement noise are chosen as $w(t) = [1, 1, 1, 1, 1, 1, 1, 1]^T \times 10^{-3}$ and $v(t) = [10^{-3}, 10^{-4}, 10^{-4}]^T$, respectively.

In the first 7 seconds of the simulation, the actual value of the sprung mass parameters is the norm value as shown in Table 1. During the next 7 seconds, the value of the sprung mass parameters increases by 1,5 times and then reduces by 2 times in the remaining time compared to the norm values. The initial value of the sprung mass parameters before estimating is set at 2 times the norm values.

Table 1. Actual vehicle parameters.

Description	Symbol	Value	Unit
Sprung mass	m_s	5394	kg
Roll moment of inertia	J_x	4600	kgm ²
Pitch moment of inertia	J_y	19632	kgm ²
Front un-sprung mass	m_{uf}	266	kg
Rear un-sprung mass	m_{ur}	427	kg
Front suspension damping coefficient	$k_{s1,2}$	7733	Ns/m
Rear suspension damping coefficient	$k_{s3,4}$	9804	Ns/m
Front suspension stiffness	$c_{s1,2}$	177000	N/m
Rear suspension stiffness	$c_{s3,4}$	193844	N/m
Front wheel stiffness	$c_{u1,2}$	493211	N/m
Rear wheel stiffness	$c_{u3,4}$	986422	N/m
Wheel damping coefficient	k_{ui}	0	Ns/m
Distance from front wheel to the vehicle center of gravity	l_f	2,400	m
Distance from rear wheel to the vehicle center of gravity	l_r	1,685	m
Distance between 2 front wheel tracks	$2t_f$	1,705	m
Distance between 2 rear wheel tracks	$2t_r$	1,495	m

4.1. Simulation Results

Simulations performed with different values of the KBF measurement covariance \mathbf{R} and process covariance \mathbf{Q} show that the convergence time and noise reduction effect depended significantly on the noise variance of the states and measurements. The lower the value of \mathbf{R} compared to \mathbf{Q} , the better the convergence time and noise reduction effect.

The time history of the estimated vertical, roll, and pitch velocity and the inertia parameters of the sprung mass for the case of measurement covariance $\mathbf{R} = \text{diag}([5 \times 10^{-5}, 5 \times 10^{-4}, 5 \times 10^{-4}])$ and process covariance $\mathbf{Q} = \text{diag}([1, 1, 1, 1, 1, 1])$ are depicted in Figure 5 and Figure 6, respectively. The thin-dark lines denote the estimated signals and bolt-light lines represent the actual signals.

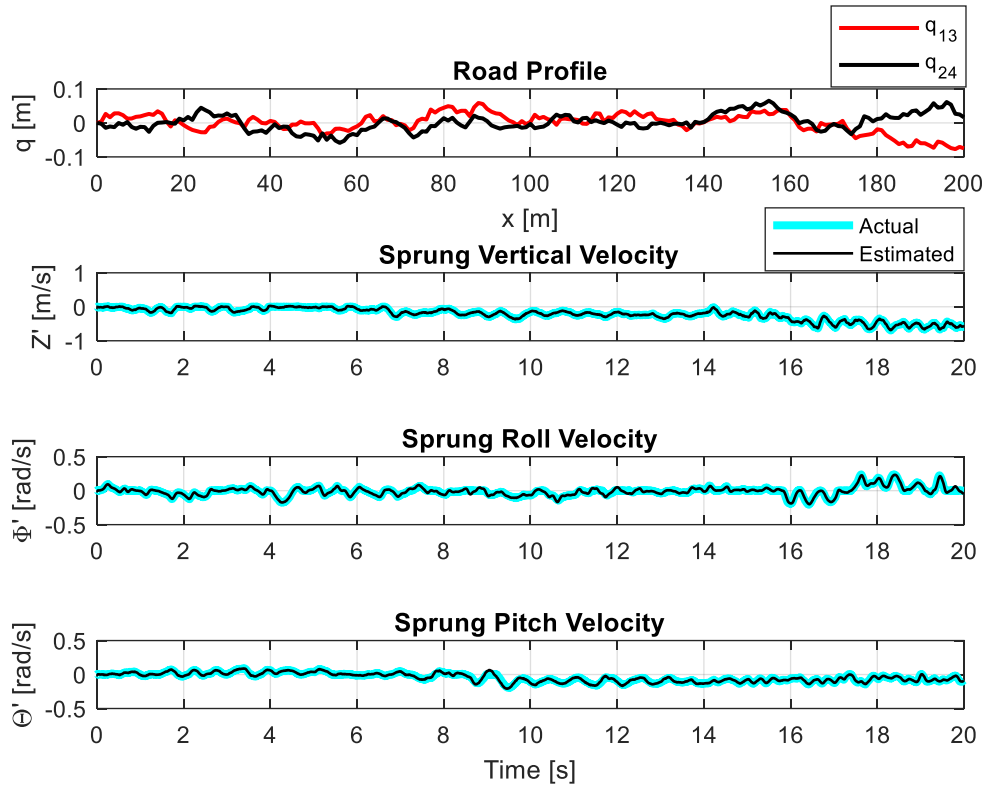


Figure 5. Estimated and actual outputs for random roughness road.

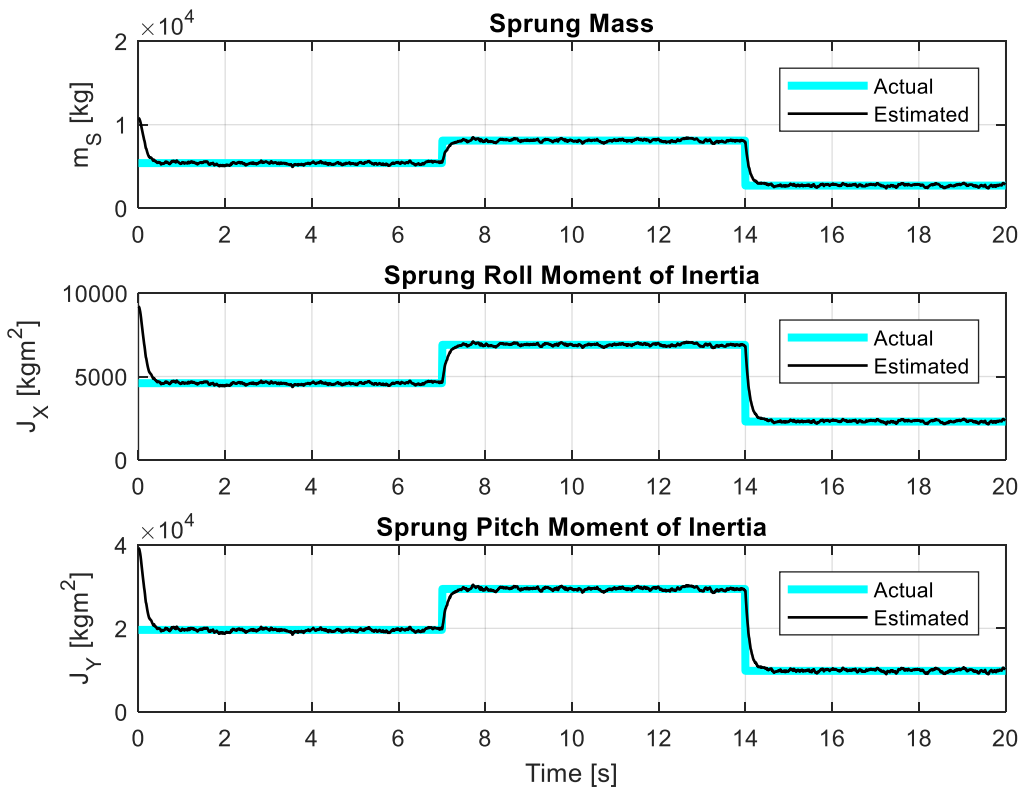


Figure 6. Estimated and actual inertia parameters of the sprung mass.

4.2. Evaluation

The accuracy of the estimator is evaluated through the root mean square error (RMSE) and mean absolute percentage error (MAPE) according to the following formula:

$$RMSE = \sqrt{\frac{1}{n} \sum_{i=1}^n (y_i - \hat{y}_i)^2}, \tag{10}$$

$$MAPE = \frac{1}{n} \sum_{i=1}^n \left| \frac{y_i - \hat{y}_i}{y_i} \right| 100\%,$$

where $y_i(t)$ is the actual parameter received from the 7 DOF spatial model, $\hat{y}_i(t)$ denotes the estimated parameter obtained by the KBF algorithm, and n stands for the total number of estimations made.

The errors between the estimated and actual parameters calculated in Table 2 show that a high accuracy estimated result can be obtained with the KBF algorithm applied to vertical, roll, and pitch velocity of sprung mass estimation.

Table 2. Estimated velocity and inertia parameter errors of the sprung mass.

Parameters	\dot{Z} (m/s)	$\dot{\Phi}$ (rad/s)	$\dot{\Theta}$ (rad/s)	m_s (kg)	J_x (kgm ²)	J_y (kgm ²)
RMSE	0,007	0,014	0,012	509,4	566,7	1829,5
MAPE	3,50 (%)	1,21 (%)	0,851 (%)	4,18 (%)	3,29 (%)	3,51 (%)

5. CONCLUSIONS

Based on a 7 DOF spatial vehicle model, the paper proposed a 3 DOF simplified model to design an estimator of vehicle inertia parameters, including mass and moments of inertia of the sprung mass. This model allows to simplify the determination of input signals for the estimator and allows the elimination of the impact of random factors from the road surface. Since the unsprung mass of the vehicle does not change during operation, the value of vehicle inertia parameters for control systems can be determined easily by estimating the inertia parameters of the sprung mass.

The parameter estimator is designed based on the Kalman–Bucy filtering algorithm applied to linear systems that change continuously over time. The working quality of the estimator is evaluated by simulation using Matlab Simulink software. The simulation results and error evaluation for a random roughness road excitation showed that the estimated parameters quickly converged to the actual value after a time of 0,5 seconds with an error of less than 10%. This allows theoretically confirming the efficiency and accuracy of the designed Kalman–Bucy estimator compared to other estimation methods.

REFERENCES

[1]. Kanwar Bharat Singh, Saied Taheri, Integrated State and Parameter Estimation for Vehicle Dynamics Control, International Journal of Vehicle Performance, 5 (2019) 329-376.
 [2]. W. Li, H. Li, K. Xu, Z. Huang, K. Li, H. Du, Estimation of Vehicle Dynamic Parameters Based on the Two-Stage Estimation Method, Sensors, 21(11) (2021) 3711. <https://doi.org/10.3390/s21113711>
 [3]. Moustapha Doumiati, Ali Charara, Alessandro Victorino, Daniel Lechner, Vehicle Dynamics

- Estimation using Kalman Filtering - Experimental Validation, John Wiley & Sons, Inc., (2013).
- [4]. N. Kidambi, R.L. Harne, Y. Fujii, G.M. Pietron, K.W. Wang, Methods in Vehicle Mass and Road Grade Estimation, SAE Int. J. Passeng. Cars – Mech, Syst., 7 (2014) 981-991. <https://doi.org/10.4271/2014-01-0111>
- [5]. A. Vahidi, A. Stefanopoulou, H. Peng, Recursive Least Squares with Forgetting for Online Estimation of Vehicle Mass and Road Grade: Theory and Experiments, Vehicle System Dynamics, 43 (2005) 31-55. <https://doi.org/10.1080/00423110412331290446>
- [6]. Daeil Kim, Seibum B. Choi, Jiwon Oh, Integrated Vehicle Mass Estimation Using Longitudinal and Roll Dynamics, The 12th International Conference on Control, Automation and Systems, Korea, (2012) 862-867.
- [7]. Y. Zha, X. Liu, F. Ma, C. Liu, Vehicle State Estimation Based on Extended Kalman Filter and Radial Basis Function Neural Networks, International Journal of Distributed Sensor Networks, 18 (2022). <https://doi.org/10.1177/15501329221102730>
- [8]. Nguyen Tuan-Anh, Nguyen Cong Tuan, Real-time Vehicle Inertial Parameters Estimation Based on a Simplified Half-Car Vertical Vibration Model. International Conference on Engineering Research and Applications ICERA 2018, LNNS, Springer, 63 (2019) 521-531.
- [9]. Wanmin Li, Yan Wang, Yaping Zhang, Yunzi Yang, Kalman Filter Method Based Vehicle Mass Estimation for Automobile Suspension System, International Journal of Circuits, Systems and Signal Processing, 13 (2019) 344-351.
- [10]. J. Kolansky, C. Sandu, Real-time Parameter Estimation Study for Inertia Properties of Ground Vehicles, The Archive of Mechanical Engineering, 60 (2013) 7-21.
- [11]. Truong Manh Hung, Vu Van Tan, Designing a Kalman–Bucy State Estimator for a Full Vertical Car Model, Mathematical Problems in Engineering, 2023 (2023). <https://doi.org/10.1155/2023/6941084>
- [12]. O. Donatus, O. Uchenna, K. K. Uka, I. B. Okafor, I. A. Amaefule, Implementation of Kalman-Bucy Filter for Continuous Time State Estimation in Simulink, International Research Journal of Advanced Engineering and Science, 3 (2017) 11-13.
- [13]. Peter Můčka, Simulated Road Profiles According to ISO 8608 in Vibration Analysis, Journal of Testing and Evaluation, 46 (2018) 405-418.